Properties of Polyethersulfone Ultrafiltration Membranes Modified With Polyethylene Glycols

Mercedes L. Méndez,[1] Analía I. Romero,[1] Verónica B. Rajal,[1,2] Elza F. Castro,[1] José I. Calvo,[3] Laura Palacio,[3] Antonio Hernández[3]

[1] *Facultad de Ingeniería – UNSa – Instituto de Investigaciones para la Industria Química, CONICET – CIUNSa Av., Bolivia, 5150 c/p 4400, Salta, Argentina*

[2] *Fogarty International Center, University of California at Davis, Davis, California*

[3] *SMAP, Paseo Belén 7, Campus Miguel Delibes, Universidad de Valladolid, 47071 Valladolid, Spain*

Polyethersulfone ultrafiltration membranes have been prepared using polyethylene glycols (PEGs) of 400, 1000, and 10,000 gmol, as additive with dimethylacetamide as solvent. Infrared analysis proves that PEG leaves almost completely the surface of the membranes after 24 h of water immersion. Scanning electron microscopy, contact angle, and liquid–liquid displacement porometry have been used to characterize the membrane morphology, surface hydrophilicity and porous structure. The relative flux reduction factor, flux, retention—of PEG (20,000 and 35,000 g/mol) and bovine serum albumin (67,000 g/mol)—and pure water permeability have been measured for the membranes. Results show that the addition of PEG increases slightly hydrophilicity and decreases pore size and narrows the corresponding pore size distribution while thickening the skin layer, in spite of the fast disappearance of the added PEG form the membrane surface. The resulting flux and pure water permeability are higher when middle size PEGs are added but decrease again when very high molecular weight (MW) PEGs are added. Retention decreases initially for increasing MWs of PEG although for very long PEG chains (MW of 10,000 g/mol) retention increases again. After filtration, the membranes with PEG added showed a lower relative flux reduction that decreases for increasing MW of the added PEGs. © 2013 Society of Plastics Engineers. POLYM. ENG. SCI., 54:1211–1221, 2014. © 2013 Society of Plastics Engineers

INTRODUCTION

Ultrafiltration (UF) membranes usually present anisotropic structures with a thin finely porous surface layer or skin, which gives selectivity to separate water and microsolutes from macromolecules and colloids. This active layer is commonly supported on a much more open macroporous substrate providing mechanical strength [1]. Asymmetric UF membranes are generally made using the phase inversion technique. The final structure of the membrane is modified by controlling a series of parameters of the process [2–4].

Both polysulfone (PSf) and polyethersulfone (PES) are poly(arylene ether sulfone)s showing excellent heat stability, oxidative resistance, optical transparency, and good solubility [5, 6]. These characteristics are supposed to arise from a high resonance effect of the sulfone groups in the polymers [5]. Because of their excellent physicochemical properties and their good membrane forming performances, PSf and PES are important membrane materials widely used in water treatment, hemodialysis, and juice concentration [7–10], for example. PES of relatively high molecular weight (MW) forms membranes with high pure water flux and low rejections [11].

The structure of the membrane is one of the key factors that affect membrane performances in UF. The configuration of the pores, and especially the pore size distribution, has to be analyzed in order to understand retention. The membrane structure and its chemical nature or charge, are also relevant because they determine the physicochemical interaction between the solute and the membrane.

However, the intrinsic hydrophobicity of PES and PSf is one of the causes of membrane fouling [10, 12, 13]. In effect, hydrophobicity and roughness play important roles in the appearance of fouling, which is the main drawback

Correspondence to: Antonio Hernández; e-mail: tonhg@termo.uva.es
Contract grant sponsor: ANPCyT; contract grant number: PICTO 36716; contract grant sponsor: CIUNSa; contract grant number: 1469/0; contract grant sponsor: Junta de Castilla y León (to Spanish authors); contract grant numbers: VA324A11nd GR18.
DOI 10.1002/pen.23637
Published online in Wiley Online Library (wileyonlinelibrary.com).

of UF membranes and, in general, of all membrane processes, since it leads to a drastic reduction in the membrane life span. The modification of the hydrophilicity of the membranes is a simple and effective method to solve the problem [14–18].

One of the possibilities to control the properties of the membrane is the use of an additive in the polymeric casting solution. There are several additives with different effects on the membrane permeability and selectivity [3, 4, 19, 20]. Various recent researches use additives to alter the shape, size and number of pores and to modify the chemical nature of the membrane surface and/or matrix [21–23] in order to develop improved membranes. However, depending on the polymer, solvent and conditions used in the preparation method, together with the additive used in the casting solution, very different effects on pore size, porosity and macrovoids formation are observed [4].

The use of polymeric additives with a hydrophilic effect is extensive. Among others: polyethylene glycol (PEG), polyvinylpyrrolidone (PVP) [19–22], or polyethylene oxide-b-polypropylene oxide-b-polyethylene oxide (Pluronics®, Plu) [4], can be used.

Numerous investigations have been performed using PEG as additive because it is highly compatible with PES having very similar solubility parameters [24, 25]. PEGs have also a pore-generation effect and when they are not overdosed give strong and mechanically resistant structures [18, 26]. However, considerable contradictory results regarding its effects on final membrane structure have been reported [, 27–31].

PES UF membranes using PEG, PVP, and Pluronics as additives were studied by Susanto and Ulbrich [4]. They found that the effect of PEG in membranes was an increase in the surface hydrophilicity, a decrease in the relative flux reduction, RFR, and a significant increase in the resistance toward adsorptive fouling when compared with the membranes without additive. Membranes with Pluronics showed the best performance and stability. Idris et al. [28] made asymmetric PES UF membrane with PEGs of MWs 200, 400, and 600 g/mol. They reported that membranes with PEG 600 showed higher pure water permeation, larger pores, and higher molecular weight cutoff (MWCO). By atomic force microscopy analysis, they observed that the membrane surface became rougher when PEGs with increasing MWs were added.

Liu et al. [29] prepared PES hollow fiber membranes with PEG 400 and water in the casting solution in order to obtain membranes with higher pure water flux. They found that PEG/solvent ratio controlled pure water flux while PES concentration did not have noticeable influence. They concluded that macrovoids were not suppressed by the addition of PEG alone, because the MW of PEG was too low. However, PEG addition in adequate amounts increased the viscosity of the polymer solution and the interconnectivity of pores.

Chakrabarty et al. [27] investigated the effect of the MW of PEG and the nature of the solvent on the morphology and permeation characteristics of PSf membranes. They found that the average pore size was not very much affected by the MW of the additive in contradiction with the results obtained by Idris et al. [28].

Another study related to the effect of PEG as a modifier of the membrane structure affecting the permeation properties was carried out by Kim and Lee [30]. These authors related the changes in permeability to kinetic and thermodynamic properties of the phase inversion process.

In summary there are somehow contradictory results in the literature concerning the effect of an addition of PEGs to PES membranes. It seems clear that an addition of PEG increases the surface hydrophilicity consequently increasing the resistance toward adsorptive fouling, decreasing RFR, when compared with the membranes without additive; but the specific effect on the membrane morphology: pore size distribution, active membrane thickness etc., is still an open question. A detailed study of the morphological changes of PES membranes when PEGs with a reasonably wide range of MWs are added is our aim here. The changes in pore size will be analyzed with a relatively new and powerful tool as the liquid–liquid displacement technique which is especially suited for an analysis of porosity of UF membranes.

In this work we have studied the effect of the addition of PEG with increasing MW (400, 1000, and 10,000 g/mol) on the structure and performance of PES UF membranes using *N-N*-dimetylacetamide (DMAc) as solvent and water as nonsolvent. Scanning electron microscopy (SEM), contact angle (CA), liquid–liquid displacement porosimetry (LLDP), Fourier transform infrared spectroscopy (FTIR), and Raman spectroscopy have been used to determine membrane structural properties while water permeation and UF experiments of bovine serum albumin (BSA) and PEG solutions were used to asses membrane performances.

EXPERIMENTAL

Materials

Commercial PES provided by BASF with an average MW of 51,000 g/mol has been used as received for the membrane solution casting. Some other data of the PES used are given in Table 1. The polymer was dried at 60°C for at least 1 day before being used in the membrane fabrication. The solvent has been DMAc purchased from Tedia Company. The non-woven Viledon 2430 support was kindly supplied by Freudenberg Vliesstoffe KG, Germany. PEGs (Merck) with MWs of 400, 1000, and 10,000 g/mol have been used as additives.

BSA with a MW of 67,000 g/mol, bought from Fluka and PEG with MWs of 20,000 and 35,000 g/mol, purchased from PH EUR, have been ultrafiltered. Other chemicals used to determine concentration of PEGs, were sodium iodide (NaI), barium chloride ($BaCl_2$), iodine (I_2),

 DOI 10.1002/pen

TABLE 1. Some manufacturer's data on the PES used.

Ultrason® E 6020 P from BASF. Typical values at 23°C		
Property	Procedure	Value
Density	ISO 1183	1.37 g/cm^3
Viscosity number (in solution: 0.01 g/mL phenol/ortho-dichlorobenzene 1)	ISO 307	82 mL/g
Glass temperature, T_g		225°C
Tensile modulus of elasticity	ISO 527-2	2700 MPa
Molecular weight [light scattering in N-methyl-2-pyrrolidone (NMP)]		51,000 g/mol
M_w/M_n [weight to number average molecular weight; gel permeation chromatography in dimethylformamide (DMF)]		3.5

and hydrochloric acid (HCl) purchased from Berna, Cicarrelli, and Mallinckrodt Chemicals, respectively.

Fabrication of the Membranes

Polymeric membranes have been prepared using the phase inversion technique induced by immersion–precipitation [1]. PES was dissolved (20% wt) in DMAc. PEGs of different MWs (400, 1000, or 10,000 Da; 20% wt) were added to the PES solution. The different membranes prepared are described in Table 2 . Each DMAC solution of PES (with the corresponding PEG) was stirred at 60°C for about 24 h until the solution became homogeneous. A solution without additive was also prepared to make a control membrane. All solutions were kept for one day in an oven at 40°C to eliminate bubbles. Afterward the solution was cast on a glass support to form a film of about 300 μm in thickness. The solvent was evaporated for 30 s at room temperature and humidity (25 ± 2°C and 50 ± 5%, respectively). The membrane was kept in the water immersion bath (25 ± 1°C) for 15 min and then washed to eliminate the solvent. Finally, the membranes were stored in deionized water until used. Some small portions of membrane were air-dried after immersion in ethanol and hexane solvents for further characterization.

Morphological Characterization

Scanning Electron Microscopy. Cross-sections of the membranes have been observed using a scanning electron microscope from JEOL (JSM 6480 LV). The dried samples were fractured, in liquid nitrogen, sputtered with a thin layer of gold and then mounted on the sample stand. Accelerating voltages of 20 kV with magnifications from 250 to 1500× have been used.

Liquid–Liquid Displacement Porosimetry. The technique chosen to determine the size distribution of the pores is the LLDP technique that has been shown to preserve the structure of the membrane [32].

The LLDP technique is a nondestructive method combining the bubble pressure technique with the measurement of liquid permeability. The technique can give fast and accurate information on permeability and pore size distribution without altering the structure of the membrane. All these advantages lead to an increasing use of this technique to perform porosimetric analysis of UF membranes [33, 34].

LLDP consists, basically, in using a liquid (wetting one) from a pair of immiscible liquids to wet the membrane so that this liquid penetrates all the pores in the membrane structure. Then, the flow of the other liquid (displacing one) is increased step by step and the corresponding equilibrium pressure measured. Among the range of possible liquid pairs to be selected [32], we chose a mixture of isobutanol and water (1/1, v/v) with a surface tension γ_{LL} = 1.9 mN/m at 25°C.

In this case, we have used the isobutanol rich phase as the wetting liquid, while the aqueous phase has been used to push the organic one out of the wetted membrane. More details on mixture preparation and experimental setup can be seen elsewhere [32]. Each equilibrium pressure value has been registered after each flux increment. The radii (r_p) of the pores opened at each applied pressure were calculated using the Cantor's equation:

$$r_p = \frac{2\gamma_{LL}}{\Delta p} \tag{1}$$

Δp is the applied pressure and γ_{LL} is the interfacial tension at the liquid–liquid interface in the pores. *Equation 1* is valid if a zero CA is assumed between the membrane surface and the wetting liquid.

By increasing the applied pressure stepwise, corresponding pore radii and flow values—represented as the permeability of the membrane (L_i = flow/pressure)—are

TABLE 2. Composition of the casting solutions.

	Additive (wt%)			Solvent (wt%)
Membrane	PEG 400	PEG 1000	PEG 10,000	DMAc
PES	—	—	—	80
P400	20	—	—	60
P1000	—	20	—	60
P10,000	—	—	20	60

The PES concentration was 20 wt% in all the cases.

obtained. Therefore, by measuring the equilibrium pressure drop, corresponding to each increment of water flux, a pore size distribution of the membrane can be evaluated. Consecutive values of differential permeability are obtained in intervals given by:

$$dL_i = \left(\frac{L_i - L_{i-1}}{L_{\text{tot}}}\right) \tag{2}$$

L_{tot} is the final permeability measured for the sample and corresponds to the permeability once all the wetting fluid has been pushed out of the pores.

If cylindrical pores are assumed, the Hagen–Poiseuille equation can be used to translate permeability pore size distributions to pore number size distributions. This correlates the volumetric flow, Q_i, of the pushing liquid with the number of pores, n_k ($k = 1, \ldots, i$) having pore radii, r_k ($<r_i$). In these terms, the corresponding measured volume flow is correlated with the number of pores opened up to the pressure step, Δp_i, by:

$$Q_i = \Delta p_i \left(\frac{\pi}{8\eta l}\sum_{k=1}^{i} n_k r_k^4\right) \tag{3}$$

where η is the dynamic viscosity of the displacing fluid and l is the pore length, which would roughly correspond to the membrane thickness in the case of symmetric membranes, while for asymmetric ones, it is approximately the active layer thickness [35].

Cutoff Estimation. Once we have done the porosimetric analysis of a sample, we can use the obtained distribution of pore sizes to estimate the MW cutoff of such a membrane. This procedure, described in a previous work [36], is based on assuming that a molecule with a size equal to the pore size which is bigger than the 90% of the pores should give a retention coefficient of a 90%. To convert sizes into MWs for the test molecule, an empirical correlation taken form literature [36], can be used.

Physicochemical Characterization

FTIR and Raman. Attenuated total reflectance ATR-FTIR and Raman spectra of membrane films have been measured using a Spectrum GX FTIR device with a high sensitivity Raman accessory from Perkin Elmer. The effect of the presence of the additive and its MW on the chemical composition of the membrane surface and its bulk should affect the peaks corresponding to the main groups of PEG in FTIR and Raman spectra, respectively.

Contact Angle. CA measurements have been done at ambient temperature using a goniometer from Ramé-Hart Instruments (Standard Goniometer with DROP Image Standard, model 200-00). This device uses a microneedle to deposit a deionized water drop (10 μL) on the membrane surface and to measure the resulting CA and the surface tension at the solid–liquid interface.

The surface energy of the polymer is estimated from the CA by means of the equipment software, using an iterative procedure proposed by Neumann. Five measurements on different points of the membrane have been performed and averaged.

Functional Characterization

The hydraulic permeability, L_p, experiments have been made in a tangential flux UF device. It consists in an acrylic cell (built in our laboratory) where the flat membrane sample is placed (effective transference area of 39.2 cm^2), a peristaltic pump (APEMA), and a reservoir containing the feed (2.5 L) and a permeate container. The permeate vessel is placed on a digital balance (Shimadzu) connected to a computer in order to register the mass flux of permeate versus time.

The experimental protocol follows the next steps: (1) first the membrane is washed with deionized water for 10 min; (2) then it is placed in the membrane cell and the system is pressurized at 200 kPa for 1 h; the relative flux reduction RFR, is calculated as the initial pure water flux divided by the steady state pure water flux; and (3) the mass fluxes, at different transmembrane pressures (ranging from 50 to 200 kPa), are measured under steady state condition as

$$J_v = \frac{Q}{A\Delta t} \tag{4}$$

J_v (m/s) is the pure water flux, Q (m^3) is the volume of water permeate, A (m^2) is the effective membrane area, and Δt (s) is the sampling time. From the slope of the linear relationship between the pure water flux J_v and the transmembrane pressure Δp, the hydraulic permeability, L_p, is calculated as:

$$L_p = \frac{J_v}{\Delta p} \tag{5}$$

Solute Transport. UF experiments of different aqueous solutions have been conducted to evaluate the influence of the MW of the additive on the performance of the membrane made. PEGs of two MWs (20,000 and 35,000 g/mol) and BSA (67,000 g/mol) aqueous solutions of 1 g/L have been ultrafiltered under a pressure of 150 kPa. PEGs were dissolved in distilled water (1 g/L) and BSA in water buffered with acetic acid at pH 5.0 (1 g/L). This pH corresponds to the protein isoelectric point; therefore, BSA is neutral in these conditions. The solute transport test was made after the membrane pure water permeability determination without taking the membrane out of the cell. The solutions were permeated separately, starting with the solute with the higher MW.

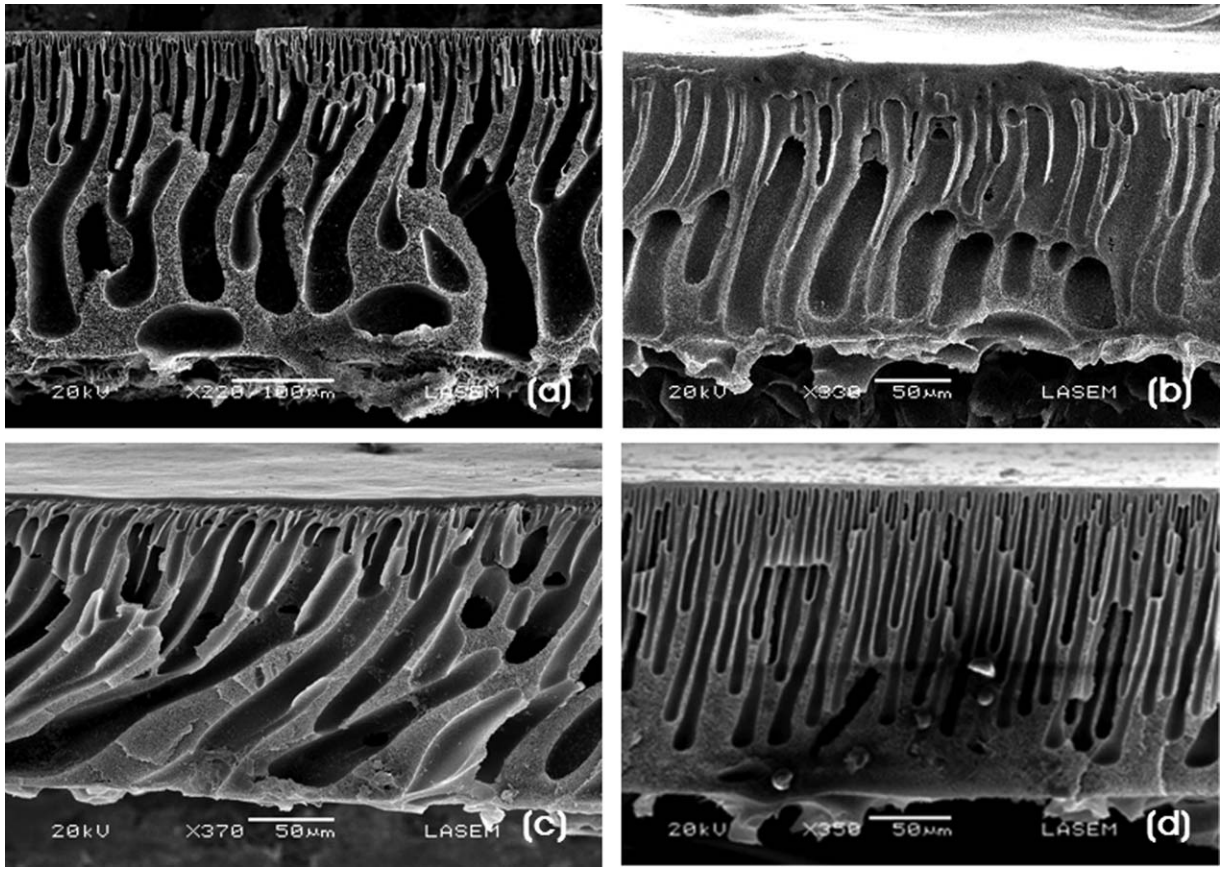

FIG. 1. Scanning electron micrographs of cross-section membranes: (a) membrane without additive, (b) with PEG 400, (c) with PEG 1000, and (d) with PEG 10,000.

A sample (5 mL) of each feed solution and another of permeate after an hour of filtration (time enough to reach stationary conditions) were extracted and their concentrations determined. The concentrations of PEG and BSA have been determined using an UV-Spectrophotometer (Genesys 10 UV, Spectronic Unicam), at 535 and 280 nm, respectively, following the method described by Sabde et al. [37].

The relative reduction of permeate flux, RFR, has been determined as the flux after 1 h of filtration (in stationary conditions) divided by the initial one. Finally, the membranes have been washed after each solute filtration for 1 h with distilled water. The apparent solute rejection, R_a, was calculated using

$$R_a\,(\%) = \left(1 - \frac{C_p}{C_f}\right) \cdot 100 \tag{6}$$

The relative flux reduction, RFR, is,

$$\mathrm{RFR}\,(\%) = \left(\frac{J_i - J_f}{J_i}\right) \cdot 100 \tag{7}$$

C_p and C_f are the solute concentrations in (g/L) at the permeate and feed membrane interfaces respectively, and J_i and J_f are the fluxes of pure water before and after the solute exposition.

RESULTS AND DISCUSSION

Morphological Study

Scanning Electron Microscopy. Cross-sectional SEM images (see Fig. 1) showed how the porous structure of the membrane changes due to the presence of the additive of different MWs in the membrane formulation. The membrane clearly includes a substrate formed by large finger-like cavities which actually should not have any role in the transport but that should give mechanical strength to the membrane. There is also a top active layer with much shorter and narrower pores, hardly visible in these images. The formation of an asymmetric morphology with a macroporous supporting structure is due to a fast instantaneous phase separation, as already noted in the literature [29–31], due to the high mutual affinity between DMAc and water and the limited compatibility of the polymer with water.

There are strong changes when PEG is added although the general asymmetric structure, as shown in Fig. 1, is

TABLE 3. Active layer thickness of the membranes.

Membrane	PES	P400	P1000	P10,000
Active layer thickness (μm)	6.1 ± 0.6	4.1 ± 0.3	5.5 ± 0.4	22.0 ± 1.8

preserved. In effect, the porous sublayer of the membrane without additive (Fig. 1a) presents larger macropores and is thicker than when PEGs are added. The finger-like shape of the pores of the substrate changes when PEGs with different MW are included. Narrower fingers are actually obtained when the MW of the additive increases. In addition, the presence of large macropores or voids in the substructure is reduced, In Fig. 1d, for example, it could be observed that the macroporous cavities are almost substituted by a bunch of closely parallel fingers. This leads to a lower relative flux reduction, RFR, as will be confirmed below probably caused by a lower tendency to a partial collapse or compaction of the structure of the porous sublayer because the finger-like structure penetrating through the membrane favors the mechanical resistance of the membrane. Similar phenomena have been observed in other studies with the same additive and different base polymer and/or solvents [31].

SEM images with magnifications over those shown in Fig. 1 (approximately 1500×) of randomly chosen areas of the membrane can also be used (after the adequate statistical treatment) to determine the mean thickness of the active layer for each membrane type. According to the so obtained thicknesses, shown in Table 3, it seems clear that there is a tendency to get thicker active layers when PEGs with higher MW are added. Although the thickness of the PES membrane without any PEG added is bigger than those for the membranes containing low MW PEGs.

Both the morphology and cross-section structure closely depend on thermodynamic parameters and kinetic of phase inversion phenomenon, so these phenomenon and exchange rate of solvent/nonsolvent in coagulation bath should control them. Roughly speaking, all the morphological effects of the addition of PEGs could be explained by the hindered diffusion of the longer PEG chains. In effect, when the casting solution is introduced to the nonsolvent bath, a rapid outlet of the solvent into the bath is produced leading to an accumulation of polymer near the surface. When the PEG molecules are small they easily spread with the solvent resulting in a thinner skin layer, whereas the larger chains reach the surface with difficulty while aggregation happens allowing the formation of a thicker skin layer and narrower pores. The process is also slowed by the increased water–polymer affinity induced by the presence of longer chains of PEG, leading again to thicker skin and denser support layers [31, 38, 39].

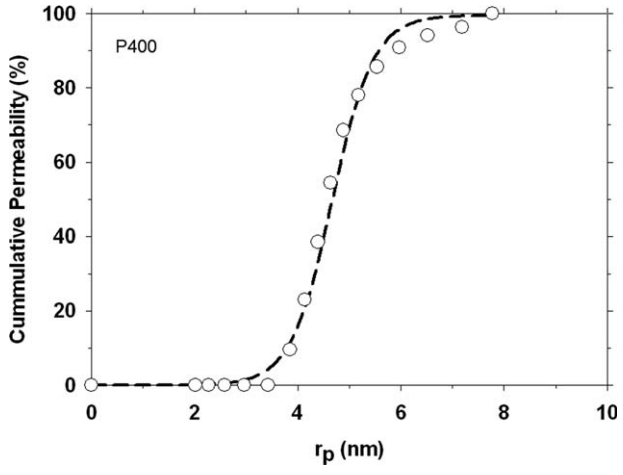

FIG. 2. Cumulative permeability distribution for membranes prepared with addition of PEG 400.

Liquid–Liquid Displacement Porosimetry. Figure 2 shows the cumulative permeability distribution (as percentage of the final permeability) for a membrane with PEG of an MW of 400 g/mol. This and similar runs show that lower pressures are required to push out the wetting liquid from the membrane pores as PEGs of increasing MW are added.

From the differential permeability distributions, the pore number distributions can be obtained by applying the Hagen–Poiseuille model for convective flows. In this procedure, the corresponding thickness, as measured from SEM pictures and shown in Table 3, have been used. The mean pore sizes as obtained from the pore number distributions and their dependency on the MW of the additive are shown in Fig. 3.

In this figure, the number mean pore sizes are also compared with the mean pore sizes obtained from the permeability distributions. Of course mean pore sizes from number distributions are slightly lower for each membrane than those obtained from permeability distributions because it is known that small contributions to permeability can be caused by a big amount of very narrow

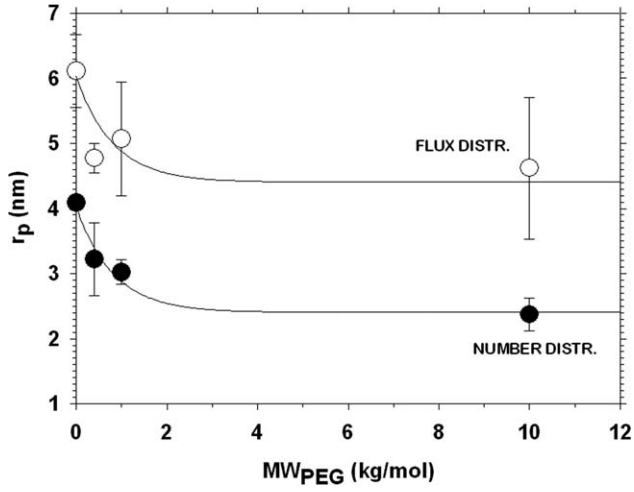

FIG. 3. Mean LLDP pore size, obtained from both permeability distribution and pore number one, as a function of the molecular weight of added PEG.

 DOI 10.1002/pen

TABLE 4. Porosimetric results from LLDP for all the analyzed membranes.

Membrane	$r_{p,mean}$ (flow distribution; nm)	$r_{p,mean}$ (pore number distribution; nm)	Pore density (10^{15} m^{-2})	Porosity (%)	Molecular weight cutoff (MWCO; kg/mol)
PES	6.1 ± 0.5	4.1 ± 0.3	5.5 ± 0.4	22.0 ± 3	60.3 ± 4
P400	4.8 ± 0.3	3.2 ± 0.3	2.9 ± 0.2	12.9 ± 2	33.6 ± 2
P1000	5.1 ± 0.5	3.0 ± 0.2	3.4 ± 0.3	12.5 ± 3	18.7 ± 2
P10,000	4.6 ± 0.5	2.4 ± 0.2	8.9 ± 0.6	11.9 ± 1	8.4 ± 0.4

pores. In any case, it is clear that higher MW of PEG results in decreasing mean pore sizes.

The main parameters obtained from LLDP analysis are shown in Table 4 for each membrane analyzed. Data in the last column correspond to the estimation of MWCO, following the procedure explained above from the pore number distributions.

These estimated weight cutoffs have been plotted as a function of the MW of the added PEG, in Fig. 4. There it can be seen that there is a very regular decrease in the resulting MWCO when bigger PEG molecules are added in the membrane formulation.

In summary, it seems clear that the addition of PEG results in a plain decrease in the mean pore size of the resulting membrane and correspondingly to a lower MWCO. These results are in accordance with those found by Chakrabarty et al. [27] for membranes of PSf. It seems clear that the resulting pores in the skin layer are narrower as the MW of the added PEG increases, leading to membranes exhibiting lower MWCO.

Physicochemical Analysis

CA Measurements. The stationary CA and surface tension values for the membranes studied are shown in Fig. 5. As expected, the incorporation of PEG as additive increases the surface hydrophilicity, starting from the relative hydrophobicity of PES without any PEG added. The values of CA reported in other publications for nonporous films of PES are around 76° [40]. The slightly lower value (67°) obtained by us for our PES is surely due to the combined effects of high porosity and roughness [1, 41]. Lower effective CAs (with an associated increase in surface tension) were obtained when PEG was added.

As usually happens with hydrophilic additives [19, 23, 27] their molecules could be occluded or entrapped between the polymer (PES in our case) chains. This effect is more obvious as the MW of the additive increases because of its hindered diffusion, as commented above. This phenomenon can explain the relatively slow decrease in the CA when large PEG molecules are added, as seen in Fig. 5.

FTIR and Raman Analysis. sence of PEG in the membranes. The infrared (IR; FTIR) spectra of PES polymeric films as well as for those with PEG added are shown in Fig. 6. The characteristic IR absorption bands of PES are observed in all the spectra. The bands at 1578 and 1486 cm^{-1} correspond to the C–H bond and C[dbond]C bond stretch in the aromatic system. Strong absorption at 1242 cm^{-1}, corresponding to the aromatic ether (C–O–C) groups, is also clearly observed [4, 42, 43]. The absorption band at 1152 is due to symmetric stretches of the sulfonyl group (SO_2) [44]. The characteristic strong absorption bands of PEG at 1117 and 1150 cm^{-1}, corresponding to C–O and C–C stretching [45], are also found in Fig. 6.

These results suggest that PEG incorporated in the membranes should be partially removed or its movement

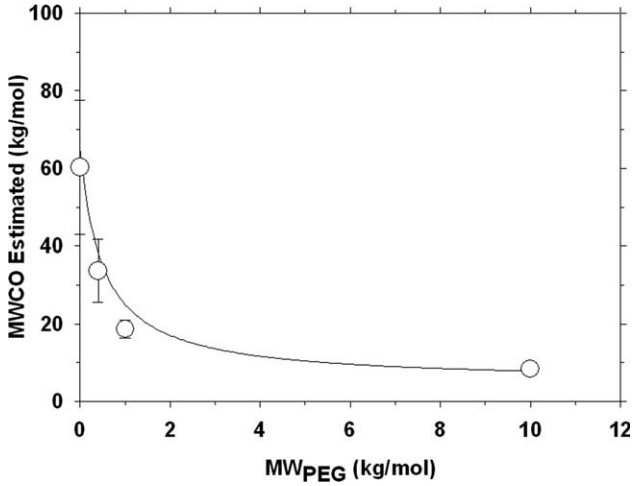

FIG. 4. Estimated molecular weight cutoff of the fabricated membranes as a function of molecular weight of PEG added.

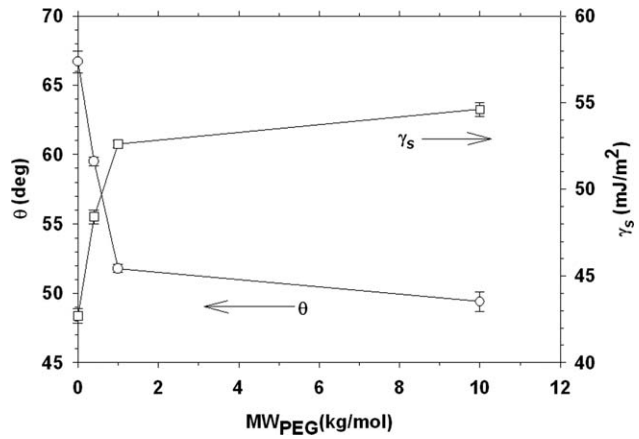

FIG. 5. Dependence of contact angle and surface tension as a function of the molecular weight of the added PEG.

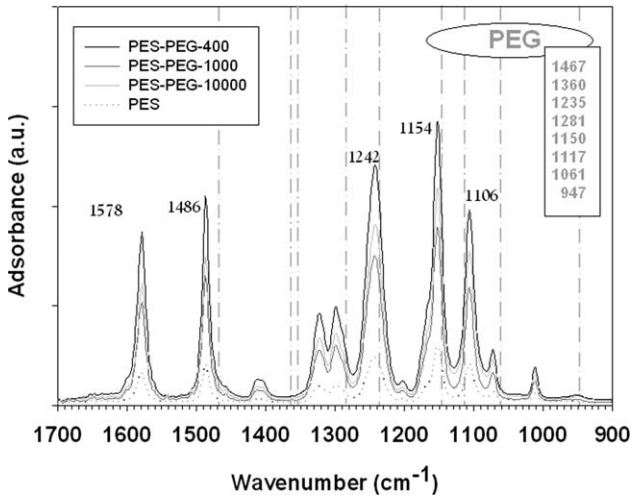

FIG. 6. FTIR spectrum of membranes prepared without additive and with the different PEGs added: PEG 400, PEG 1000, and PEG 10,000. Vertical lines correspond to wave numbers characteristic of PEG.

restricted on the membrane surface when they have been soaked for more than 24 h [46]. Although FTIR absorbance peaks for PEG are quite close to those presented by PES as shown in Fig. 6, it seems clear that PEG should be absent from, or present in a very small proportion on, the surface of the membrane. In order to test whether PEG is actually being lost with increasing water immersion of the membranes, we prepared several membranes with PEGs with different MWs but with only 3 min of immersion in water. As can be seen in Fig. 7, for membranes prepared with PEG 10,000, the 1467, 1343, and 1280 cm^{-1} absorption bands corresponding to CH_2 scissoring, wagging and twisting vibrations of PEG [47], are more intensely observed in the spectrum of the 3 min soaked membrane. The above mentioned characteristic strong peaks of PEG (1117 and 1150 cm^{-1}) can also be observed along with weak peaks at 1061 and 947 cm^{-1}, corresponding to C–O and C–C stretching and CH_2 rocking [47]. This confirms that the changes in the IR spectrum of PEG on the surface of the membranes should be attributed to its interaction with water.

In conclusion, FTIR results are compatible with the presence of only small amounts of the added PEG on the membrane surface but they seem to imply that there is a partial, or even almost total, loss of the PEG chains on the surface of the membranes when they are soaked for more than 24 h. It is known [3, 19], that the chains of the hydrophilic additives could be occluded or entrapped between the PES molecules, the effect being stronger for larger added molecules. The shorter PEG chains could be lost with the solvent in the coagulation bath, as mentioned. These factors could in part explain the apparent shrinkage of PEG from the surface of the membranes.

According to some Refs. [4, 19, 31, 48], it is quite difficult to lose the added PEG from the membrane matrix, and even more when the MW is high. To analyze the presence of PEG in the membrane bulk, the Raman technique has been used. From the analysis of the spectra of the membranes with added PEGs, we can conclude that slight modifications appear in the bands of the main

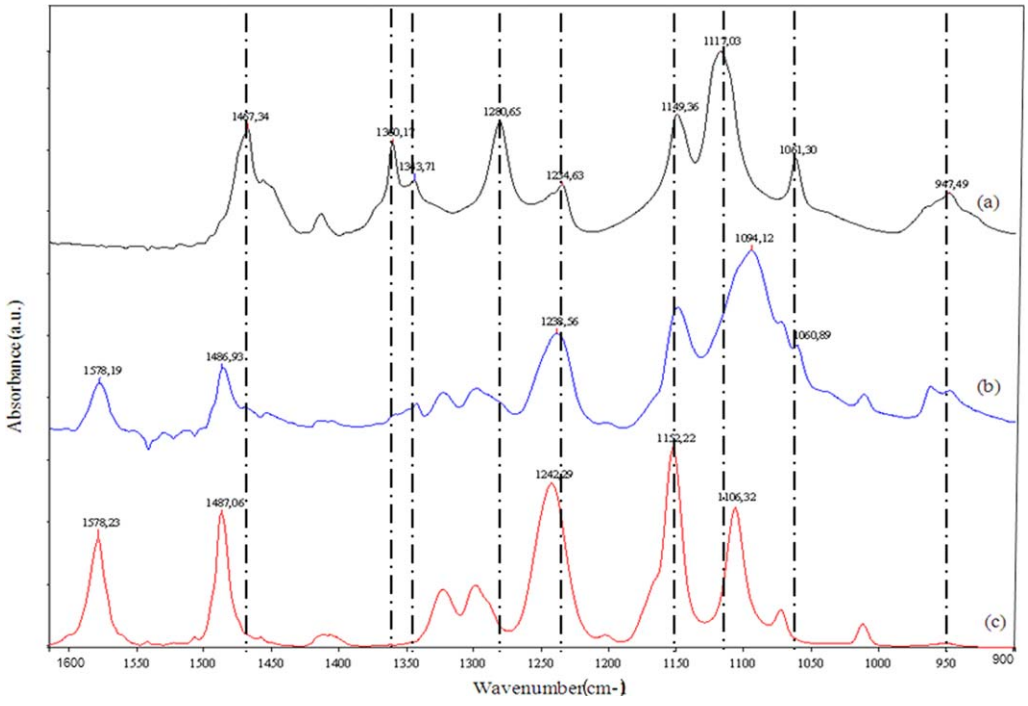

FIG. 7. FTIR spectrum of PEG 10,000 g/mol (a) and membranes prepared with molecular weight of PEG (10,000) and 3 min (b) and 24 h (c) of soaking, respectively. Vertical lines correspond to the peaks of PEG. [Color figure can be viewed in the online issue, which is available at wileyonlinelibrary.com.]

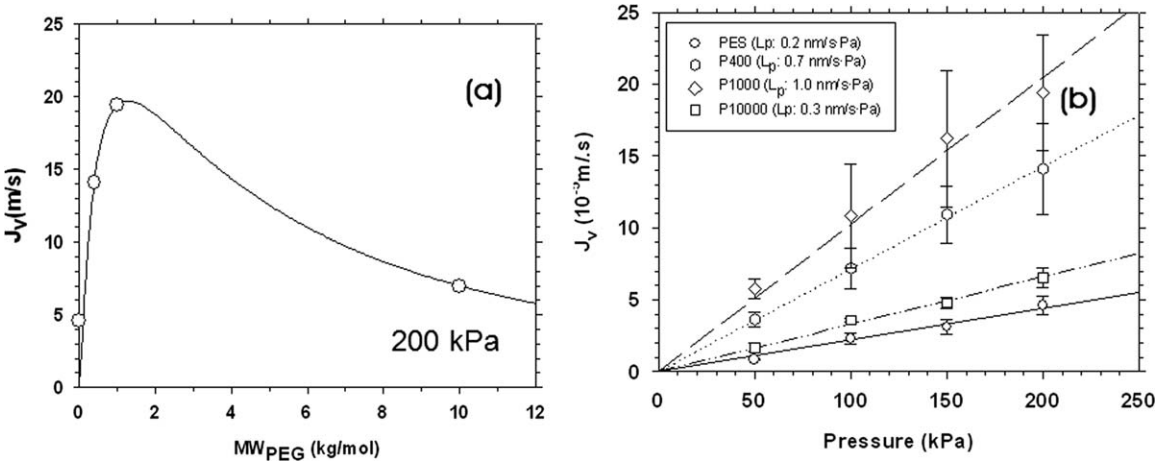

FIG. 8. (a) Permeate flux (J_v) for maximum applied pressure (200 kPa). (b) Pure water permeabilities, $L_p \times 10^9$ (m/Pa s).

functional groups of PES [21] (compared to the spectra of the membrane without additive). These modifications could be attributed to the contribution of PEG, confirming that there is PEG trapped within the PES matrix of the membrane even after long water immersions although the corresponding amount is quite difficult to quantify.

Permeation Experiments

Flux and Permeability. To determine the performance of the membranes, they were characterized in terms of the permeation of pure water. This has been done attending to their: flux, hydraulic permeability and rejection for different solutes, namely: PEGs of 20,000 and 35,000 g/mol and BSA of 65,000 g/mol.

Flux and pure water permeability obtained are plotted in Fig. 8. They are higher for all the membranes with additive as shown in Fig. 8a and b, which is a desirable feature in UF of aqueous solutions. Flow and permeability increase for the membranes with PEGs with increasing MWs up to 1000 g/mol. For PEG 10,000 these magnitudes decrease to figures close to those found for the PES membranes made without any added PEG. This decrease could be explained by the results obtained in LLDP, because these membranes have both the smallest pore size and the lowest overall porosity. This in turn can be related to the SEM images, where it was seen that the skin layer of the membranes made with added PEG of 10,000 g/mol has a significantly greater thickness. The combination of all these factors leads to an increase in the hydraulic resistance and consequently a noticeable decrease in the permeability for these membranes. The presence of shorter PEG molecules increases hydrophilicity without increasing too much the thickness of the skin layer or decreasing the pore size thus increasing permeability (as seen in Tables 3 and 4).

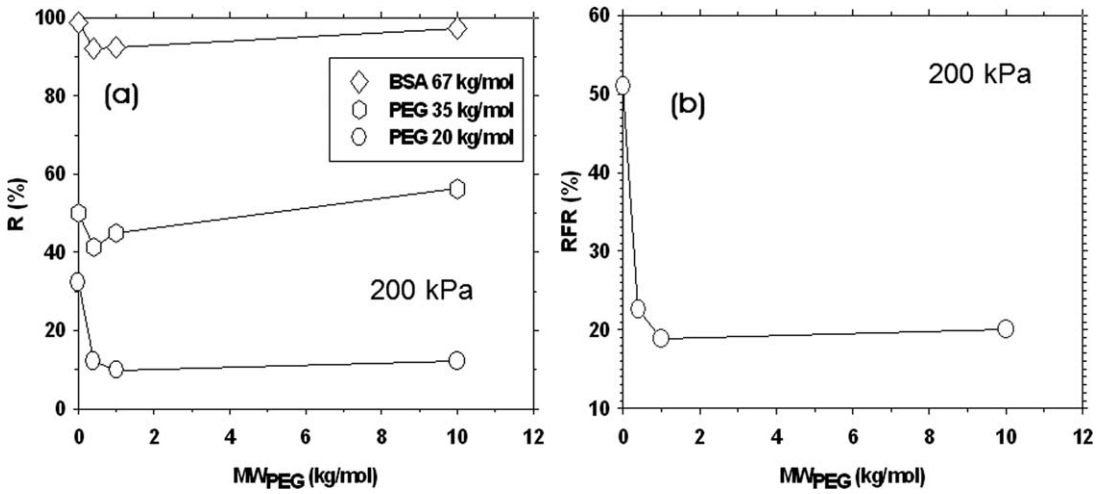

FIG. 9. (a) Retention coefficients for the solutes studied and (b) relative flux reduction for the maximum applied pressure (200 kPa).

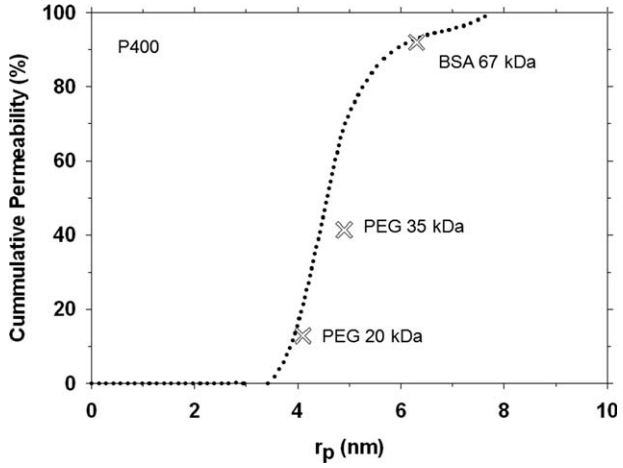

FIG. 10. Cumulative permeability distribution for membranes prepared with addition of PEG 400. The corresponding retentions for PEGs of 20 and 35 kg/mol and BSA are shown too.

Solute Retention and RFR. Figure 9a shows the retention curves of the solutes studied (PEG 20,000, PEG 35,000, and BSA). The retention coefficient (R) is maximal when no PEG is added probably due to the high level of membrane fouling due to the relative low hydrophilicity. When the MW of PEG increases retention increases as well. For membranes with PEG 10,000, R reaches values that are comparable or higher than those for the membrane without added PEG. These results are as expected considering the pore size and MWCO estimation of the membranes obtained from LLDP porometry because, in effect, the membranes with PEG 10,000 have the lowest pore size and MWCO, besides having a narrower pore size distribution that makes it more selective.

The level of fouling of the membranes are characterized by their relative water flux reduction (RFR), see Fig. 9b. This coefficient resulted to be a 50% for the non PEG membrane while it decreased below 20% when PEG was added.

The membranes with added PEG have greater resistance to fouling absorption as compared with membranes without any additive according to their increased hydrophilicity confirmed by the CA results previously described.

These results agree with other studies for hydrophilic additives [3, 21]. RFR values do not change significantly with MW of the additive; this could be due to the relatively low effect of the MW of the added PEG on porosity and pore radius of the membranes.

Finally, the retention coefficients shown in Fig. 9a can be compared with the distributions obtained from LLDP with a very good accordance if the molecular size of the solutes tested are taken into account [49, 50]. As an example this comparison is shown in Fig. 10 for the membrane with PEG of 400 g/mol.

CONCLUSIONS

The presence of PEGs of different MWs as additives affects considerably the performance and morphology of PES UF membranes. From SEM images we could observe that the incorporation of PEG modifies the membrane structure. The increase in the MW of the added PEG produces a reduction of the size and a change in the shape of the macropores in the porous support of the membrane, making them more finger-like shape. The thickness of the active layer for membranes with added PEG 10,000 increased significantly.

Results of LLDP showed that pore radius decreases with the MW of the added PEG while the number of pores is reduced and the pore size distribution becomes narrower. These parameters have a close relationship with permeability and solute retention. This is due to the ability of this method to detect exclusively active pores, i.e., those opened and thus controlling the transmembrane transport.

The flux and pure water permeability are higher for membranes with PEG, in spite of their decrease in pore radii, due to the increase in hydrophilicity caused by the additive. In the case of the 10,000 g/mol PEG, the effect of the reduction in pore size and porosity on permeability is too strong and cannot be balanced by the increase in hydrophilicity. The retention coefficient, R, decreases when longer PEGs are used. When a PEG of 10,000 g/mol is added, R increases probably due again to the effect of lower pore radii and porosity that overcome the effect of the increase in hydrophilicity.

Moreover, the membranes with additive have a RFR below a 20%. For membranes without PEG, this parameter is somewhat over 50%. This indicates that the addition of PEG increases the resistance to fouling caused by the increased hydrophilicity in these membranes. It is also important to take into account that the fouling tendency decreases (decreasing RFR) as the MW of the added PEG increases. This would explain the initial steps of decreasing retention finally overtaken by the effect of the pore size reduction.

In summary the addition of PEG to PES UF membranes clearly increases its hydrophilicity and decreases fouling. They decrease the pore size and increase the thickness of the skin layer. The balance of all these effects leads to optimal permeability, flux and RFR when medium size PEGs (here of around 1000 g/mol) are added to PES UF membranes. It seems clear that ulterior increases of the MW of the added PEG harms or do not affect significantly the performances obtained for PEGs with MWs around 1000 g/mol.

ACKNOWLEDGMENT

The authors thank Freudenberg Vliesstoffe KG, Germany, for providing the Viledon 2430 no-woven support.

REFERENCES

1. M. Mulder, Basic Principles of Membrane Technology, Kluwer Academic Publishers, Dordrecht (1991).

2. C.A. Smolders, A.J. Reuvers, R.M. Boom, and I.M. Wienk, *J. Membr. Sci.*, **73**, 259 (1992).
3. I.M. Wienk, R.M. Boom, M.A.M. Beerlage, A.M.W. Bulte, C.A. Smolders, and H. Strathmann, *J. Membr. Sci.*, **113**, 361 (1996).
4. H. Susanto and M. Ulbricht, *J. Membr. Sci.*, **327**, 125 (2009).
5. Y.K. Han, S.D. Chi, Y.H. Kim, B.K. Park, and J.I. Jin, *Macromolecules*, **28**, 916 (1995).
6. J.H. Botkin, R.J. Cotter, M. Matzner, and G.T. Kwiatkowski, *Macromolecules*, **26**, 2372 (1993).
7. M.I. Dova, K.B. Petrotos, and H.N. Lazarides, *J. Food Eng.*, **78**, 431 (2007).
8. B. Jiao, A. Cassano, and E. Drioli, *J. Food Eng.*, **63**, 303 (2004).
9. K.-i. Yamamoto, M. Matsuda, M. Hayama, J. Asutagawa, S. Tanaka, F. Kohori, and K. Sakai, *J. Membr. Sci.*, **272**, 211 (2006).
10. H. Yamamura, K. Kimura, and Y. Watanabe, *Environ. Sci. Technol.*, **41**, 6789 (2007).
11. C. Zhou, Z.C. Hou, X.F. Lu, Z.Y. Liu, X.K. Bian, L.Q. Shi, and L.A. Li, *Ind. Eng. Chem. Res.*, **49**, 9988 (2010).
12. M.D. Kennedy, H.K. Chun, V.A.Q. Yangali, B.G.J. Heijman, and J.C. Schippers, *Desalination*, **178**, 73 (2005).
13. H. Susanto and M. Ulbricht, *Water Res.*, **42**, 2827 (2008).
14. J. Mansouri, S. Harrisson, and V. Chen, *J. Mater. Chem.*, **20**, 4567 (2010).
15. J.Y. Park, M.H. Acar, A. Akthakul, W. Kuhlman, and A.M. Mayes, *Biomaterials*, **27**, 856 (2006).
16. Q. Yang, N. Adrus, F. Tomicki, and M. Ulbricht, *J. Mater. Chem.*, **21**, 2783 (2011).
17. Z. Yi, L.-P. Zhu, Y.-Y. Xu, Y.-F. Zhao, X.-T. Ma, and B.-K. Zhu, *J. Membr. Sci.*, **365**, 25 (2010).
18. W. Zhao, Y. Su, C. Li, Q. Shi, X. Ning, and Z. Jiang, *J. Membr. Sci.*, **318**, 405 (2008).
19. J. Marchese, M. Ponce, N.A. Ochoa, P. Prádanos, L. Palacio, and A. Hernández, *J. Membr. Sci.*, **211**, 1 (2003).
20. D.B. Mosqueda-Jimenez, R.M. Narbaitz, T. Matsuura, G. Chowdhury, G. Pleizier, and J.P. Santerre, *J. Membr. Sci.*, **231**, 209 (2004).
21. R.M. Boom, I.M. Wienk, T. van den Boomgaard, and C.A. Smolders, *J. Membr. Sci.*, **73**, 277 (1992).
22. K. Sunitha, Y.V.L.R. Kumar, and S. Sridhar, *J. Mater. Sci.*, **44**, 6280 (2009).
23. B. Chakrabarty, A.K. Ghoshal, and M.K. Purkait, *J. Membr. Sci.*, **315**, 36 (2008).
24. S. Niemela, J. Leppanen, and F. Sundholm, *Polymer*, **37**, 4155 (1996).
25. I. Pillin, N. Montrelay, and Y. Grohens, *Polymer*, **47**, 4676 (2006).
26. Y.H. Zhao, B.K. Zhu, L. Kong, and Y.Y. Xu, *Langmuir*, **23**, 5779 (2007).
27. B. Chakrabarty, A.K. Ghoshal, and M.K. Purkait, *J. Membr. Sci.*, **309**, 209 (2008).
28. A. Idris, N. Mat Zain, and M.Y. Noordin, *Desalination*, **207**, 324 (2007).
29. Y. Liu, G.H. Koops, and H. Strathmann, *J. Membr. Sci.*, **223**, 187 (2003).
30. J.-H. Kim and K.-H. Lee, *J. Membr. Sci.*, **138**, 153 (1998).
31. A. Idris and L.K. Yet, *J. Membr. Sci.*, **280**, 920 (2006).
32. J.I. Calvo, A. Bottino, G. Capannelli, and A. Hernández, *J. Membr. Sci.*, **239**, 189 (2004).
33. R.I. Peinador, J.I. Calvo, P. Prádanos, L. Palacio, and A. Hernández, *J. Membr. Sci.*, **348**, 238 (2010).
34. J.M. Sanz, R. Peinador, J.I. Calvo, A. Hernández, A. Bottino, and G. Capannelli, *Desalination*, **245**, 546 (2009).
35. S. Munari, A. Bottino, G. Capannelli, and P. Moretti, *Desalination*, **53**, 11 (1985).
36. R.I. Peinador, J.I. Calvo, K. ToVinh, V. Thom, P. Prádanos, and A. Hernández, *J. Membr. Sci.*, **372**, 366 (2011).
37. A.D. Sabde, M.K. Trivedi, V. Ramachandhran, M.S. Hanra, and B.M. Misra, *Desalination*, **114**, 223 (1997).
38. W.Y. Chuang, T.H. Young, W.Y. Chiu, and C.Y. Lin, *Polymer*, **41**, 5633 (2000).
39. B. Jung, J.K. Yoon, B. Kim, and H.-W. Rhee, *J. Membr. Sci.*, **243**, 45 (2004).
40. H. Susanto, S. Franzka, and M. Ulbricht, *J. Membr. Sci.*, **296**, 147 (2007).
41. D.Y. Kwok and A.W. Neumann, *Adv. Colloid Interface Sci.*, **81**, 167 (1999).
42. N. Bolong, A.F. Ismail, M.R. Salim, D. Rana, and T. Matsuura, *J. Membr. Sci.*, **331**, 40 (2009).
43. A.F. Ismail and A.R. Hassan, *Sep. Purif. Technol.*, **55**, 98 (2007).
44. K. Nakanishi, Infrared Absorption Spectroscopy, 2nd ed., Holden-Day, Inc., San Francisco (1977).
45. Y.-l. Su, J. Wang, and H.-z. Liu, *Langmuir*, **18**, 5370 (2002).
46. D.-y. Zuo, Y.-y. Xu, W.-l. Xu, and H.-t. Zou, *Chin. J. Polym. Sci.*, **26**, 405 (2008).
47. K. Fukushima and H. Matsuura, *J. Mol. Struct.*, **350**, 215 (1995).
48. W.-L. Chou, D.-G. Yu, M.-C. Yang, and C.-H. Jou, *Sep. Purif. Technol.*, **57**, 209 (2007).
49. E. Arkhangelsky and V. Gitis, *Sep. Purif. Technol.*, **62**, 619 (2008).
50. B. Jachimska, M. Wasilewska, and Z. Adamczyk, *Langmuir*, **24**, 6866 (2008).